The Plant Cell, Vol. 9, 355–365, March 1997 © 1997 American Society of Plant Physiologists

Molecular Dissection of the *AGAMOUS* Control Region Shows That *cis* Elements for Spatial Regulation Are Located Intragenically

Leslie E. Sieburth[1] and Elliot M. Meyerowitz[2]

Division of Biology 156-29, California Institute of Technology, Pasadena, California 91125

***AGAMOUS* (*AG*) is an Arabidopsis MADS box gene required for the normal development of the internal two whorls of the flower. *AG* RNA accumulates in distinct patterns early and late in flower development, and several genes have been identified as regulators of *AG* gene expression based on altered *AG* RNA accumulation in mutants. To understand *AG* regulatory circuits, we are now identifying *cis* regulatory domains by characterizing *AG*::β-glucuronidase (*GUS*) gene fusions. These studies show that a normal *AG*::*GUS* staining pattern is conferred by a 9.8-kb region encompassing 6 kb of upstream sequences and 3.8 kb of intragenic sequences. Constructs lacking the 3.8-kb intragenic sequences confer a GUS staining pattern that deviates both spatially and temporally from normal *AG* expression. The GUS staining patterns in the mutants for the three negative regulators of *AG*, *apetala2*, *leunig*, and *curly leaf*, showed the predicted change of expression for the construct containing the intragenic sequences, but no significant change was observed for the constructs lacking this intragenic region. These results suggest that intragenic sequences are essential for *AG* regulation and that these intragenic sequences contain the ultimate target sites for at least some of the known regulatory molecules.**

INTRODUCTION

Genetic dissection of pattern formation in many organisms has revealed complex circuitry for regulatory gene expression. For example, in flower development, the pattern of floral organs is achieved through region-specific patterns of homeotic gene activity (reviewed in Weigel and Meyerowitz, 1994). This regional activity of the homeotic genes requires initial activation by meristem identity genes and delimitation of the zone of activity through the functions of cadastral genes. One approach toward understanding pattern formation is to characterize how a gene's regulatory elements confer its temporal and spatial patterns of expression. To achieve a clearer understanding of the regulatory circuits controlling flower development, we are now identifying the DNA elements that are required to specify the normal pattern of *AGAMOUS* (*AG*) expression.

AG is an Arabidopsis MADS box gene that is required in the third and fourth whorls of developing flowers to specify the identity of the organs that arise in these two whorls (stamens and carpels, respectively) and to confer determinacy to the floral meristem (Bowman et al., 1989; Yanofsky et al., 1990). By using in situ hybridization, *AG* RNA was shown to be expressed early in flower development in the region of the floral meristem that gives rise to the third- and fourth-whorl organs (Drews et al., 1991). This early expression pattern is consistent with the proposed role of *AG* in specification of these two organs. A distinct pattern of late *AG* expression was revealed by examination of *AG* RNA accumulation in mature flowers (Bowman et al., 1991). In mature stamens, *AG* RNA is concentrated in the connective tissue; in carpels, *AG* RNA accumulates in the stigma and ovules. Young ovules show an essentially uniform *AG* expression pattern, which, as the ovules develop, becomes resolved into a single cell layer of *AG* expression in the endothelium.

In addition to the complex *AG* expression pattern observed in wild-type flowers, several different genes have been identified as regulators of *AG* based on altered *AG* RNA abundance patterns in mutant plants. For instance, both *APETALA2* (*AP2*) and *LEUNIG* (*LUG*) are negative regulators of early floral expression of *AG* in the outer whorls; plants carrying mutations of these genes show *AG* RNA accumulation in the outer whorls of the flower (Drews et al., 1991; Liu and Meyerowitz, 1995). Similarly, *CURLY LEAF* (*CLF*) is a negative regulator of vegetative *AG* expression, and in *clf* mutants, *AG* RNA accumulates in leaves (Coupland et al., 1993). The meristem identity genes *LEAFY* (*LFY*) and *APETALA1* (*AP1*) are involved in accurate activation of *AG*

[1]Current address: Department of Biology, McGill University, 1205 Avenue Docteur Penfield, Montreal, PQ H3A 1B1, Canada.
[2]To whom correspondence should be addressed. E-mail meyerowitze@starbase1.caltech.edu; fax 818-449-0756.

expression and have overlapping roles as positive regulators of *AG* (Weigel and Meyerowitz, 1993).

The combination of a complex pattern of developmental regulation of expression and many genes identified as regulators of its expression makes *AG* a candidate for studies of regulatory control elements. We have examined the ability of two overlapping regions of the *AG* gene to confer an *AG* pattern of expression on the β-glucuronidase (*GUS*) reporter gene. We present an analysis of the GUS staining patterns conferred by these two constructs in the wild type and in *ap2*, *lug*, and *clf* mutants. Results of this analysis suggest that important control regions are located within a transcribed region of the gene that is primarily intronic and that additional regulators of late *AG* expression patterns in the ovule remain to be identified.

RESULTS

AG Reporter Gene Fusions

The *AG* gene contains at least nine exons and eight introns (Figure 1A; Yanofsky et al., 1990). That the sequences required for normal *AG* gene expression might not be simply within the 5′ upstream region was suggested by the lack of a phenotype for transgenic plants carrying *AG* upstream sequences fused to the *AP3* coding region (L.E. Sieburth, T. Jack, and E.M. Meyerowitz, unpublished results). The large size of intron 2 (~3 kb) made it a good candidate for the location of regulatory sequences. To test whether this region of the *AG* gene contains the sequences required to confer its normal pattern of gene expression, we assembled two gene fusions between the *AG* genomic region and the *GUS* reporter gene. The first construct, pAG-I::*GUS* (Figure 1B), contains ~6 kb of upstream sequences plus 3.8 kb of genomic sequences. The genomic region extends into exon 3 and is fused to *GUS* near the 5′ end of this exon at nucleotide 331 of the cDNA (Yanofsky et al., 1990). This fusion site was selected to preserve the intron–exon splice junction while retaining a minimum of coding sequences from exon 3. The second construct, pAG::*GUS*, is shown in Figure 1C. It contains the same 6 kb of upstream sequences as in the first construct. Because the translational start site has not been identified for *AG* (Yanofsky et al., 1990), we fused the *GUS* coding region close to the 3′ end of the first described exon (at nucleotide 91 of the cDNA). We used this fusion site to ensure the use of the usual transcriptional and translation start sites for *AG*, and differences in expression (GUS staining) patterns between the two constructs should have been due only to the presence and/or absence of intron 1, intron 2, and exon 2.

Each construct was introduced into Arabidopsis ecotype Nossen (No-0). For each construct, GUS staining patterns were examined in at least 10 lines of independent transformants. Although variation in the intensity of staining was observed among lines carrying a given construct, the patterns of GUS staining were indistinguishable. Subsequent detailed analyses used the transgenic line pGUS1.4a for the pAG::*GUS* construct and 635c2 for the pAG-I::*GUS* construct. Occasionally, some individuals from two of the transgenic lines carrying the pAG-I::*GUS* construct displayed a strong *ag* mutant phenotype. We were unable to detect GUS staining in these plants, suggesting that the mutant phenotype is the result of a cosuppression phenomenon (reviewed in Dougherty and Parks, 1995) rather than of an activity of the pAG-I::*GUS* gene fusion product.

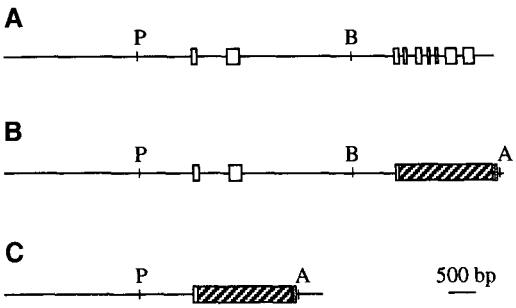

Figure 1. *AG* Genomic Structure and *AG* Reporter Gene Fusions.

(A) The genomic structure of *AG*. Boxes depict exons.
(B) Schematic representation of the pAG-I::*GUS* gene fusion, which is fused at the 5′ end of the third exon. The diagonally striped box represents the *GUS* gene. The stippled box at right represents the 3′ nopaline synthase terminator.
(C) The pAG::*GUS* gene fusion, which is fused near the 3′ end of the first exon. *GUS* is represented by the diagonally striped box, and the 3′ nopaline synthase terminator is represented by the stippled box at right.
P, B, and A denote restriction sites for PstI, BamHI, and Asp718, respectively.

GUS Staining Patterns in Intact Tissue

Seedlings stained for GUS activity are shown in Figure 2A. The seedling on the right contains the pAG-I::*GUS* construct and shows no GUS staining. Because *AG* RNA has not been detected in the vegetative tissues of wild-type plants, this lack of GUS activity is consistent with the pAG-I::*GUS* construct conferring a normal *AG* expression pattern. A GUS-stained seedling carrying the pAG::*GUS* construct is shown at the left in Figure 2A. GUS staining, readily apparent in the leaf blades and in the stem, suggests that this construct lacks at least some *AG* regulatory control elements.

GUS-stained inflorescences of plants carrying the pAG::*GUS* and the pAG-I::*GUS* constructs are shown in Figures 2B and 2C, respectively. GUS staining was not detectable in the young floral buds of plants carrying the pAG::*GUS* construct (Figure 2B), and in the older flowers,

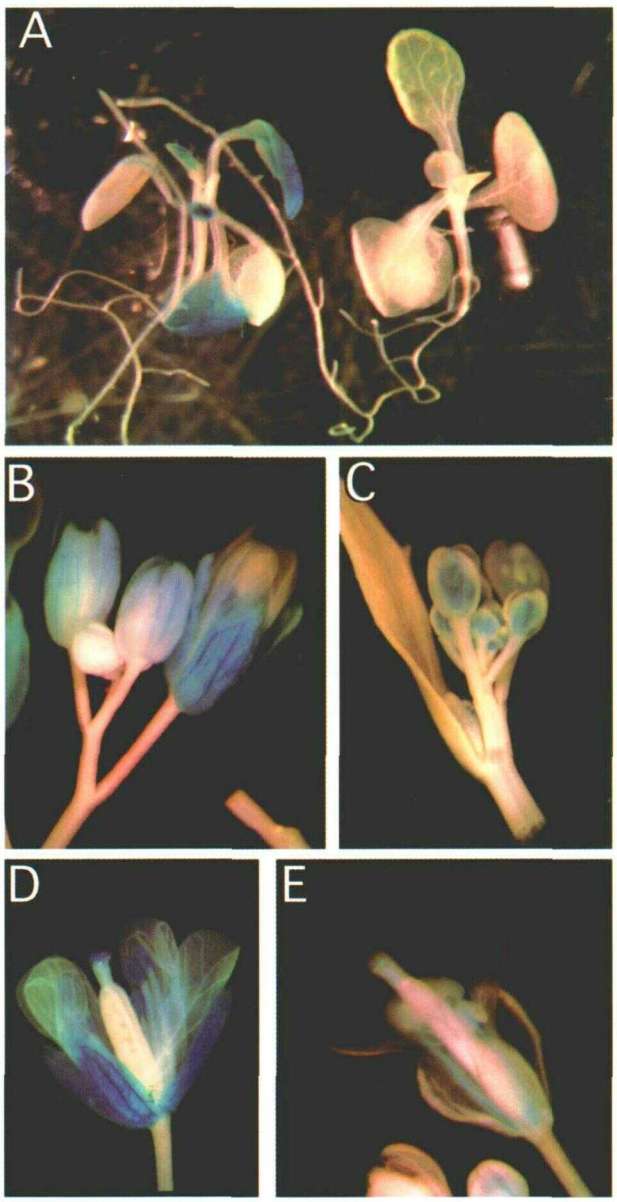

Figure 2. GUS Staining Patterns of Whole Tissue of Transgenic Arabidopsis (No-0) Plants.

(A) Fourteen-day-old GUS-stained seedlings. The seedling at left carries the pAG::*GUS* transgene, and the seedling at right carries the pAG-I::*GUS* transgene.
(B) Inflorescence from a plant carrying the pAG::*GUS* transgene.
(C) Inflorescence from a plant carrying the pAG-I::*GUS* transgene.
(D) Flower from a plant carrying the pAG::*GUS* transgene.
(E) Flower from a plant carrying the pAG-I::*GUS* transgene.

the staining product was most prominent in the sepals. In contrast, inflorescences from plants with the pAG-I::*GUS* construct showed intense GUS staining in very young buds (Figure 2C). In situ hybridization of *AG* RNA shows the most intense signal in very young floral buds, starting with stage 3 flowers (Drews et al., 1991). Thus, the staining pattern for the pAG-I::*GUS* construct matches our expectations of an *AG* expression pattern. A stained flower at anthesis (stage 13; for stage 13 and all subsequent floral stages, refer to Smyth et al., 1990) from a pAG::*GUS* plant is shown in Figure 2D, and a flower from a pAG-I::*GUS* plant is shown in Figure 2E. The flower carrying the pAG::*GUS* construct showed intense staining in the sepals, the anthers, and the stigma, whereas the flower from a plant that contained the pAG-I::*GUS* construct lacked staining in the sepals but displayed a small amount of staining in a few regions of the stamens and carpels. Because in the wild type, *AG* RNA is restricted to the third and fourth whorl of the flower, only the pAG-I::*GUS* construct appears to confer a GUS staining pattern that reflects normal *AG* RNA distributions. The differences between these staining patterns suggest that spatial, temporal, and quantitative aspects of *AG* gene expression require intragenic sequences.

Detailed Analysis of GUS Staining in Plants Carrying pAG::*GUS* and pAG-I::*GUS*

Examination of GUS staining in intact tissue provides only a generalized idea of the reporter gene expression pattern. To define these patterns in cellular detail, inflorescences that were histochemically stained for GUS activity were embedded in paraplast and sectioned. Figure 3 shows GUS staining patterns observed for plants containing the pAG-I::*GUS* construct. Under dark-field illumination, the particulate staining product appears as reddish dots on the greenish white background of unstained tissue. An inflorescence meristem, along with stage 2, early stage 3, and stage 5 flowers, is shown in Figure 3A. No staining was seen in the inflorescence meristem or the stage 2 flower. The early stage 3 flower shows a small amount of staining in the central part of the floral meristem, and the stage 5 flower shows intense staining throughout the central part of the flower. In Figure 3B, the stage 3 and stage 4 flowers also show GUS staining that is restricted to the region that will give rise to the third- and fourth-whorl organs. Figure 3B also includes two flowers at stage 7; the one to the right shows a small petal primordium that is not stained, and both show heavy staining in the developing stamens and carpels. GUS staining patterns in all of these flowers were indistinguishable from the pattern of *AG* RNA accumulation in wild-type flowers, as has been documented by in situ hybridization (Drews et al., 1991).

GUS staining patterns in mature flowers carrying the pAG-I::*GUS* transgene were also studied. Figure 3C shows the apex of a carpel in which abundant staining is clearly visible in the stigma along with a small amount of stain in the style.

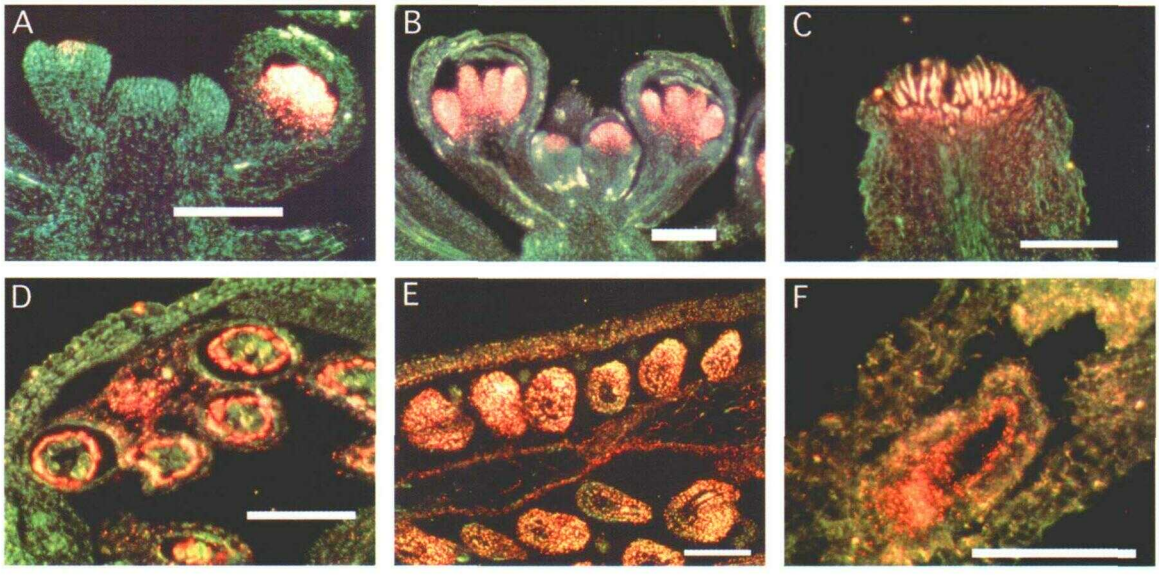

Figure 3. GUS Staining Patterns from Plants Carrying the pAG-I::*GUS* Transgene.

(A) Sections through an inflorescence meristem with stage 2, stage 3, and stage 5 flowers. GUS staining is visible only in the stage 3 and stage 5 flowers and is localized to the central region of the floral meristem.
(B) Section through an inflorescence containing stage 3, stage 4, and two stage 7 flowers. The two stage 7 flowers show abundant GUS staining that is restricted to the developing stamens and carpels and that is absent from the sepals and petal primordia.
(C) A longitudinal section of the apex of a carpel showing abundant GUS staining in the stigmatic papillae and a lower level of staining in the style.
(D) Cross-section of a stamen showing GUS staining in the connective tissue and in the tapetum but not in the developing pollen grains or in the sepal or petal.
(E) Longitudinal section of a carpel from a stage 12 flower showing essentially uniform GUS staining in the developing ovules.
(F) An ovule from a stage 14 flower showing GUS staining that is restricted to the endothelium.
Bars = 100 μm.

A cross-section of a stamen is shown in Figure 3D. Abundant staining can be observed in the tapetum and the connective tissue. Sections of carpels in Figures 3E and 3F show the GUS staining pattern observed in ovules of stage 12 and 14 flowers, respectively. Ovules of stage 12 flowers show uniform GUS staining; accumulation of the GUS staining product in the mature ovule is much more restricted, being abundant mainly in the endothelial cell layer. The ability to detect this very late pattern of GUS staining was somewhat variable. We attribute the variability to the long half-life of the GUS enzyme (Jefferson et al., 1987). This long half-life is expected to result in a lag between a decrease in RNA abundance and the corresponding decrease in GUS staining.

The patterns of GUS staining in pAG-I::*GUS* plants generally mirror those that have been documented for *AG* RNA accumulation in wild-type flowers (Bowman et al., 1991; Drews et al., 1991). One possible exception is that abundant GUS staining was observed in the tapetum of mature stamens. The question of whether *AG* is expressed in the tapetum has not been addressed previously. Our result suggests that *AG* is expressed in this tissue; alternatively, additional sequences (3′ or intragenic in the 3′ half of the gene) may be needed to repress expression within the tapetum. All of the other GUS staining results indicate that the *AG* DNA sequences included in the pAG-I::*GUS* plants are sufficient to confer the expected *AG* pattern of gene expression both early and late in development.

The staining pattern for transgenic plants carrying the pAG::*GUS* construct was also investigated in detail by examining sections of embedded, stained tissue. The inflorescence meristem did not stain for GUS, although a low level of diffuse staining was occasionally observed in the stem below the meristem, as shown in Figure 4A. No staining was detected in stage 2 flowers (Figure 4A). For stages 3 through 6, the staining pattern was somewhat variable. A diffuse and somewhat patchy GUS staining pattern first appears in stage 3 flowers; we have observed that staining is occasionally more intense in the floral meristem, but just as often it shows no spatial restriction. Figure 4A shows a stage 4 flower with a moderate amount of stain distributed in a nearly uniform pattern. Between stages 5 and 8, a punctate pattern of intensely stained cells appears in four positions

around the base of the flower, shown in a stage 6 flower in Figure 4B and a stage 9 flower in Figure 4C. These intensely staining cells appear to be centered at the junction between the sepal base and the floral meristem and extend into both the sepal and the receptacle. GUS staining in the stamens was variable in young flowers (the stage 6 flower in Figure 4B shows intense staining only in one of the two developing stamens shown in that section), but by stage 8, abundant staining is uniformly distributed throughout the stamens (data not shown). In the developing carpels, no *GUS* expression was seen until late in development (Figures 4B and 4C). No GUS staining was detectable in petals, as is shown for petal primordia (Figures 4B and 4C) and in the mature flower (Figures 2B, 2D, and 4D). GUS staining in the sepals was first detected at stage 5. At this stage, staining appeared along the apex of the lateral sepal that immediately overlays the carpel (Figure 4B) and at the sepal base. Staining becomes detectable at the apex of all the sepals in flowers between stages 5 and 9 (Figure 4C). Between stages 10 and 12, the GUS staining domain rapidly expands to encompass the entire sepal (Figure 4D).

Late in flower development, abundant GUS staining was observed in stamens of pAG::*GUS* plants. GUS staining is essentially uniform during the time of rapid stamen expansion (stages 8 to 12), except that it is largely excluded from the developing pollen grains (Figures 4C and 4D). In intact tissue, it is readily apparent that at anthesis, the level of GUS staining in the stamens is much higher in plants carrying the pAG::*GUS* transgene than in those with the pAG-I::*GUS* transgene (compare Figures 2D and 2E).

Carpels late in development showed a complex pattern of GUS staining in pAG::*GUS* plants. At stage 11, GUS staining suddenly and transiently appears in the transmitting tract (Figure 4F); this staining declines during stage 12 (data not shown). Within the ovules, GUS staining was not detected until stage 12, when it was frequently observed within the nucellus (compare Figure 4F, showing a stage 11 flower, with Figure 4G, showing a stage 12 flower). By stage 17, the

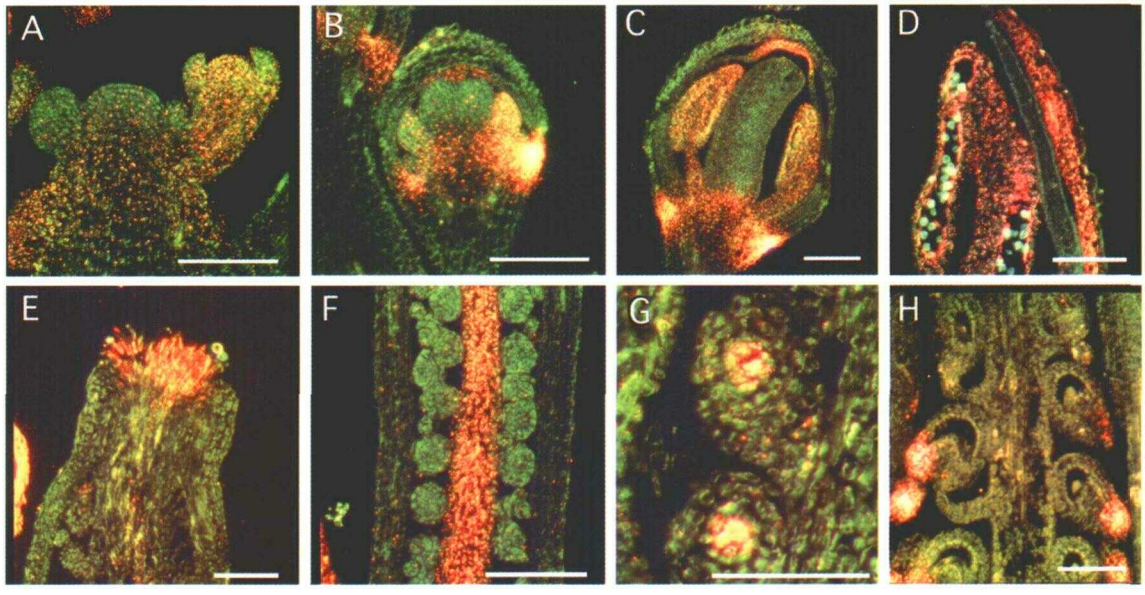

Figure 4. GUS Staining Patterns from Plants Carrying the pAG::*GUS* Transgene.

(A) Longitudinal section through an inflorescence meristem. GUS staining is not apparent in the stage 2 flower, but a low level of GUS staining is visible below the inflorescence meristem. In this section, staining is almost uniform in the stage 4 flower.
(B) An early stage 6 flower showing a small amount of staining in the apex of the sepal immediately overlaying the developing carpels. Essentially no staining is visible in the developing carpel, and variable staining can be seen in the developing stamens. Note the bright spot of staining immediately below the sepal on the right.
(C) GUS staining in a stage 9 flower showing a pattern similar to that seen at stage 6, except that the staining of the stamen is less variable.
(D) A portion of a stage 12 flower showing abundant staining in the stamen and sepal but no staining in the petal.
(E) A longitudinal section of the apex of a carpel showing staining in the stigma but no detectable staining in the style or developing ovules.
(F) A section through a carpel of a stage 11 flower. GUS staining is abundant in the transmitting tract but not in the ovules.
(G) Ovules within a stage 12 flower showing GUS staining within the nucellus.
(H) GUS staining within the stage 17 ovule is restricted to the micropylar end of the integuments.
Bars = 100 μm.

only ovular GUS staining that could be detected was in the integuments around the micropyle (Figure 4H). These patterns of GUS staining all differ from the normal *AG* RNA abundance pattern (Bowman et al., 1991; Drews et al., 1991) and the pattern of staining conferred by the pAG-I::*GUS* construct. Thus, the normal pattern of *AG* expression within the ovule must require sequences within the 3.8-kb intragenic region. In contrast, GUS staining in the stigmatic papillae and in the nectaries of both pAG::*GUS* and pAG-I::*GUS* plants (Figures 3C, 4E, and data not shown) is indistinguishable from the normal pattern of *AG* RNA abundance (Bowman et al., 1991). Thus, these two aspects of late expression must be conferred by the upstream sequences that are contained in the pAG::*GUS* construct.

GUS Staining Patterns in *ap2*, *lug*, and *clf* Mutants

The requirement for intragenic sequences to confer many elements of the normal pattern of *AG* expression led us to question whether any of the known regulators of *AG* expression act on intragenically located *cis* elements. Two negative regulators of *AG* function within the flower. In plants carrying mutations in either the *AP2* or the *LUG* gene, the onset of *AG* by expression is slightly earlier than that seen in the wild type (stage 2 versus stage 3 in the wild type; Drews et al., 1991; Liu and Meyerowitz, 1995). In strong *ap2* mutants, *AG* RNA was detected in all four whorls, whereas in strong *lug* mutants, *AG* RNA localization in ectopic positions was more variable. In *lug* mutants, *AG* RNA has been detected predominantly along the margins of first-whorl organs (Liu and Meyerowitz, 1995).

Each of the *AG* reporter gene constructs was crossed to plants with the strong mutant alleles *ap2-2* and *lug-3*, and homozygous mutants containing the transgene were obtained. If the wild-type products of these genes were to regulate *AG* by using upstream sequences, then we would expect to see an enlarged GUS staining domain for plants carrying both the pAG::*GUS* and the pAG-I::*GUS* constructs. Alternatively, if regulation by these genes were to require intragenically located *cis* sequences, then only the pAG-I::*GUS* construct would be expected to respond to the loss of the negative regulators.

Flowers from *ap2-2* pAG-I::*GUS* plants produced intense GUS staining, with the staining product appearing within 3 hr. This staining appeared at least 5 hr earlier than it did in either wild-type pAG-I::*GUS* flowers or *ap2-2* pAG::*GUS* flowers (data not shown). Figure 5A shows a section through

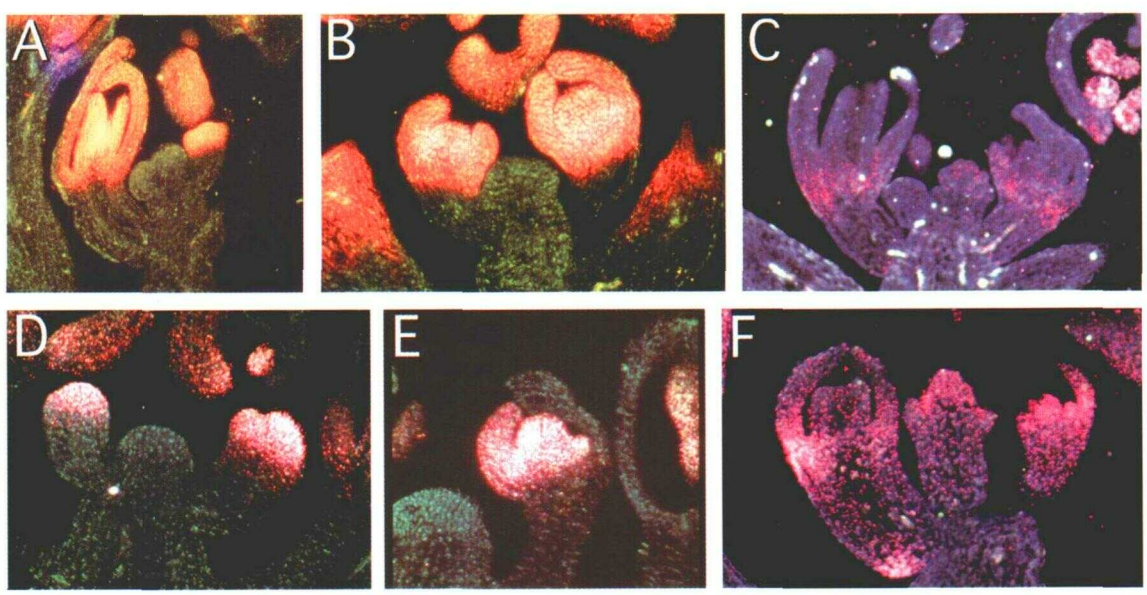

Figure 5. GUS Staining Patterns in *ap2-2* and *lug-3* Plants Carrying the pAG-I::*GUS* and pAG::*GUS* Transgenes.

(A) A section through an *ap2-2* pAG-I::*GUS* inflorescence showing stage 2, stage 3, and stage 6 flowers.
(B) Another *ap2-2* pAG-I::*GUS* inflorescence showing flowers at stages 4 and 5.
(C) A section through an *ap2-2* pAG::*GUS* inflorescence showing the GUS staining pattern in flowers at stages 2, 3, 6, and 8.
(D) The GUS staining pattern of a *lug-3* pAG-I::*GUS* inflorescence. Flowers at late stage 2 and stage 3 show abundant GUS staining throughout the floral meristem.
(E) A *lug-3* pAG-I::*GUS* flower at stage 6 showing GUS staining in one of the two sepals in this section.
(F) A section through a *lug-3* pAG::*GUS* inflorescence showing the GUS staining pattern in stage 4 and stage 6 flowers.

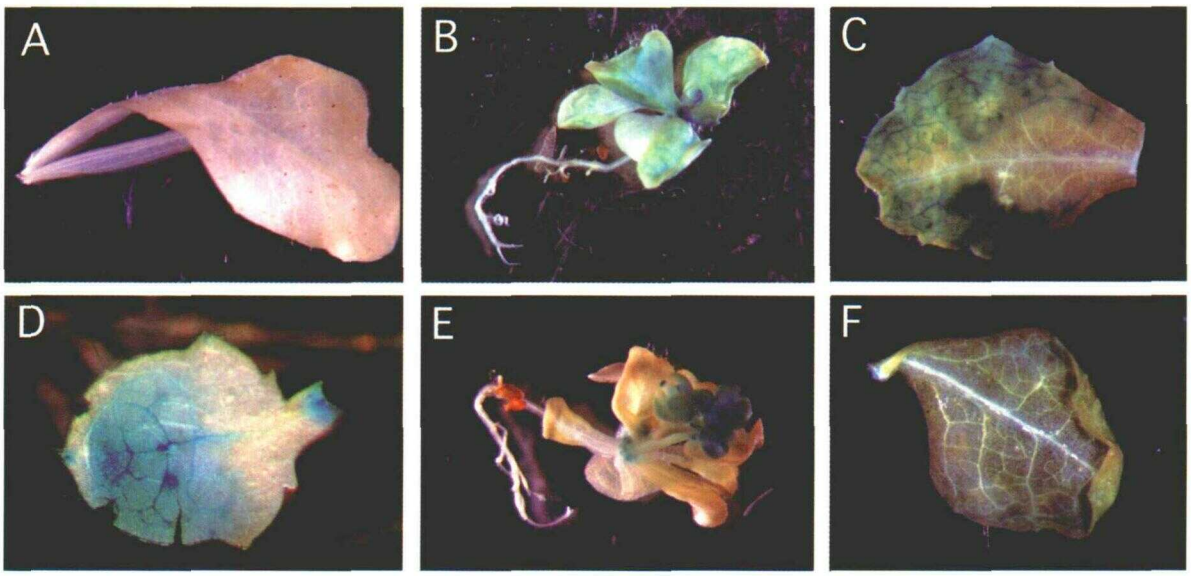

Figure 6. GUS Staining Patterns in Leaves of *clf-2* and *CLF* Plants Carrying the pAG-I::*GUS* and pAG::*GUS* Transgenes.

(A) A GUS-stained leaf from a pAG-I::*GUS* plant in which no staining is visible.
(B) A *clf-2* plant carrying the pAG-I::*GUS* transgene shows GUS staining in the leaves.
(C) A higher magnification view of a GUS-stained leaf of a *clf-2* pAG-I::*GUS* plant shows that GUS staining occurs primarily around the margins of the leaf.
(D) A GUS-stained leaf from a pAG::*GUS* plant.
(E) A *clf-2* plant carrying the pAG::*GUS* transgene.
(F) A higher magnification view of a GUS-stained leaf of a *clf-2* pAG::*GUS* plant shows a small amount of GUS staining along the curled margins of the leaf.

an *ap2-2* pAG-I::*GUS* inflorescence containing a stage 2 and early stage 3 flower. No GUS staining can be seen in the stage 2 flower, whereas the stage 3 flower has intense GUS staining throughout the floral meristem and the emerging sepal primordia. Slightly older stage 4 and stage 5 flowers are shown in Figure 5B. Abundant GUS staining is evident throughout the entire developing flowers. The staining pattern observed for *ap2-2* pAG::*GUS* flowers is shown in Figure 5C. Staining is diffuse in the developing flowers. In young flowers, it appears primarily at the base of the sepals (in a punctate pattern). In older flowers, GUS staining appears in a pattern consistent with the cell-type specific staining seen in fourth-whorl organs of the wild type (data not shown). Thus, only the pAG-I::*GUS* construct responds to the loss of the *AP2* regulator, indicating that negative regulation of *AG* by *AP2* must require DNA sequences located within the 3.8-kb intragenic region.

Similar results were obtained for *GUS* expression in *lug-3* mutants. A section containing a late stage 2 flower and a late stage 3 flower of a GUS-stained *lug-3* pAG-I::*GUS* inflorescence is shown in Figure 5D. GUS staining is evident throughout the apex of the late stage 2 flower and is clearly visible in the sepal primordia of the stage 3 flower. In the stage 6 flower shown in Figure 5E, GUS staining can be seen in the developing stamens and carpels as well as one of the sepals. In contrast, the *lug-3* pAG::*GUS* inflorescences show diffuse low-intensity staining in young flowers (data not shown). In slightly older flowers, a patchy pattern of staining that is similar to wild-type pAG::*GUS* staining is evident. In Figure 5F, a stage 4 flower shows diffuse staining, primarily in the carpel primordia. In the stage 6 flower, GUS staining appears primarily in a punctate pattern at the base of the developing sepals. These data show that only the pAG-I::*GUS* construct contains the *cis* sequences that allow a response to the loss of the *LUG* negative regulator.

CLF is another negative regulator of *AG* (Coupland et al., 1993). In plants carrying mutations in the *clf* gene, *AG* RNA is detected in vegetative organs (Coupland et al., 1993). To determine whether the *CLF* gene uses intragenic sequences for its regulation of *AG* RNA, both the pAG-I::*GUS* and the pAG::*GUS* constructs were crossed to plants carrying the *clf-2* mutation, and homozygous mutants carrying the transgenes were obtained. The GUS staining patterns observed in these plants are shown in Figure 6. Plants carrying the pAG-I::*GUS* construct do not normally show vegetative GUS staining (Figure 2A, plant at right, and Figure 6A). In a *clf-2* mutant, however, abundant vegetative GUS staining can be readily observed (Figures 6B and 6C). Plants carrying the

pAG::*GUS* transgene normally show GUS staining in leaves (Figure 2A, plant at left, and Figure 6D). In *clf-2* mutants, however, the vegetative GUS staining was slightly reduced (Figures 6E and 6F). That only the construct with the intragenic region responds to the loss of *clf* activity by gaining *GUS* expression in the leaves shows that like *AP2* and *LUG*, *CLF* uses intragenic sequences to regulate *AG* expression.

DISCUSSION

The importance of intragenic sequences for conferring a normal pattern of *AG* expression was shown by comparing two *AG*::*GUS* expression patterns. *GUS* fusion constructs that contain ~6 kb of upstream sequences and ~3.8 kb of intragenic sequences of *AG* (pAG-I::*GUS*; Figure 1B) confer a staining pattern that is indistinguishable from the wild-type *AG* in situ hybridization pattern (Bowman et al., 1991; Drews et al., 1991), except for some GUS staining seen in the tapetum. Thus, those 9.8 kb of upstream and intragenic sequences must contain all of the promoter and enhancer elements required for accurate temporal and spatial regulation of both early and late *AG* expression. To gain insight into the activities of intragenic and upstream control elements, we analyzed the GUS staining patterns that result when the intragenic region is missing.

Intragenic Sequences Are Required to Prevent Vegetative Expression

Accumulation of the GUS staining product in the vegetative tissues (leaf blades, the shoot apical meristem, and along the stem) of pAG::*GUS* plants stands out in marked contrast both to the *AG* RNA accumulation pattern in wild-type plants (Drews et al., 1991) and to the GUS staining pattern of pAG-I::*GUS* plants (Figure 1A). Because the pAG::*GUS* and the pAG-I::*GUS* transgenes differ only with respect to the 3.8 kb of intragenic sequences, one or more *cis* elements that are essential for repression of vegetative *AG* expression must lie within the intragenic region. An early flowering mutant (*clf*) with curled leaves and homeotic transformations of the first-whorl sepals to carpels and of the second-whorl petals to stamens has been described by Coupland et al. (1993). The *clf* mutant phenotype is similar to transgenic plants that ectopically express *AG* (Mandel et al., 1992; Mizukami and Ma, 1992), and *AG* RNA has been detected in the vegetative tissue of the *clf* mutant (Coupland et al., 1993). These results suggest that the 3.8 kb of intragenic sequences contained within the pAG-I::*GUS* construct may contain the *cis* elements used by the *CLF* gene product to repress *AG* expression in vegetative tissues. This suggestion was confirmed by the observation that only plants carrying the pAG-I::*GUS* transgene showed a gain of GUS staining in leaves of *clf-2* plants.

AG Expression Early in Flower Development Requires Intragenic Sequences

Both spatial and temporal control of *AG* expression in early flower development also require intragenic sequences. Plants carrying the pAG::*GUS* construct showed a variable pattern of GUS staining in early flowers that was generally of low intensity and not clearly restricted to the central region of the flower meristem (Figure 4A). This pattern is similar to the *AG* in situ hybridization pattern observed in flowers from plants carrying mutations in the genes that encode two positive regulators of *AG* expression, *ap1* and *lfy* (Weigel and Meyerowitz, 1993). These results suggest that the target sites for these two gene products might lie within the 3.8 kb of intragenic sequences that contain the pAG-I::*GUS* construct.

The spatial pattern of early *AG* expression also requires intragenic sequences, because the pattern of GUS staining in the pAG::*GUS* plants deviates from the *AG* in situ hybridization pattern (Drews et al., 1991; Figures 4A to 4C). Normally, *AG* is uniformly expressed at high levels in both the stamens and carpels, beginning at a stage before their morphological differentiation. In contrast, for pAG::*GUS* plants, GUS staining in the fourth-whorl carpels did not appear until late stage 11; yet, in the third whorl, abundant GUS staining was observed in the stamens by stage 8. These differences in third- and fourth-whorl staining patterns suggest that *AG* gene expression is controlled independently in each of these whorls. A control element (located in the upstream region) may positively regulate *AG* expression in developing stamens. The lack of GUS staining in the carpels of pAG::*GUS* plants may be a consequence of the lack of activation in the floral meristem, as described above, or it might indicate that an additional control element for positive regulation in developing carpels is located in the intragenic region. No specific candidates for genes that might serve as specific positive regulators of *AG* expression in developing stamens or carpels have been identified.

In contrast, two genes have been identified as negative regulators of *AG* expression in early flower development: *AP2* and *LUG* (Drews et al., 1991; Liu and Meyerowitz, 1995). That only the gene fusion containing intragenic sequences can respond to the loss of either of these genes (by expanding its expression domain early in development) leads to the formal conclusion that intragenic sequences are required for the regulation of AG by these two regulators. What we cannot determine from the data, however, is whether this is a direct requirement for *cis* elements located within the intragenic region. It is possible that the intragenically located domain for activation of *AG* early in flower development is a prerequisite for negative regulation, in which case the precise location of sequences used by *AP2* and *LUG* for negative regulation could reside either intragenically or upstream. Alternatively, it may be that the lack of expansion of GUS staining in the *ap2-2* pAG::*GUS* and the *lug-3* pAG::*GUS* plants reflects a direct requirement for *cis* se-

quences within the intragenic region. Precise localization of the *cis* sequences used by *AP2* and *LUG* requires a detailed mutagenesis analysis. This work is currently in progress.

Late *AG* Expression Is Complex

The GUS staining patterns of pAG-I::*GUS* and pAG::*GUS* suggest a much more complicated control of late *AG* expression in the carpel than was suspected on the basis of the *AG* in situ hybridization (Bowman et al., 1991). GUS staining was detected in the stigmatic papillae of both pAG::*GUS* (Figure 4E) and pAG-I::*GUS* (Figure 3C) plants; however, this is the only element of late *AG* carpel expression that is conserved in pAG::*GUS.* pAG::*GUS* plants lack the stylar staining that can be seen in pAG-I::*GUS* plants (Figures 3C and 4E); instead, they show transient GUS staining in the transmitting tract of stage 11 flowers (Figure 4F). Within the developing ovules, the GUS staining pattern in pAG::*GUS* plants also deviates markedly from the wild-type *AG* expression pattern (Figures 4F to 4H). No GUS staining was detected in young ovules (stages 9 to 11) at the time when in the wild type, *AG* RNA is uniformly distributed. At a slightly later stage (stage 12), strong GUS staining was detected in the nucellus (Figure 4G). This is also a transient expression pattern, and by the time the ovule had matured, the only ovular GUS staining that could be observed was in the integuments adjacent to the micropyle (Figure 4H). These results indicate that sequences upstream of *AG* contain *cis* elements that activate gene expression within the transmitting tract, nucellus, and parts of the integuments. Sequences located intragenically must be required to initiate the early ovular expression pattern and to repress expression patterns in the transmitting tract, nucellus, and integument.

The only gene that has been suggested to regulate *AG* expression during ovule development is *BELL1* (*BEL1*). This assignment as a negative regulator of *AG* is based on the observation that in *bel1* mutants, *AG* transcripts fail to accumulate specifically in the endothelium but rather remain in a uniform pattern throughout the ovule (Modrusan et al., 1994; Ray et al., 1994). More recently, it has been suggested that this effect on *AG* expression is not direct, because expression domains of *AG* and *BEL1* overlap in wild-type flowers (Reiser et al., 1995). The fact that removal of the intragenic region from the *AG*::*GUS* gene fusions results in a much more complex GUS staining pattern than mere loss of the negative regulation supports the idea that additional regulators of *AG* expression late in ovule development remain to be identified.

Evolutionary Conservation of Intragenic Control Elements

In general, *cis* elements required for gene expression are found in regions upstream (5′) from the transcriptional start site; however, it is not uncommon to find control elements located downstream (3′) of a gene as well (Dietrich et al., 1992; Larkin et al., 1993). Much less common are regulatory control elements located within a gene. In Drosophila, several genes have been identified that contain regulatory control elements within introns. For instance, the first intron of the tropomyosin 1 gene contains both positive and negative *cis*-acting elements that confer both temporal and muscle-specific expression patterns (Gremke et al., 1993). Similarly, the β3 tubulin gene contains an enhancer within its first intron that regulates expression along the anterior–posterior axis (Hinz et al., 1992).

In plants, the presence of the first intron has been correlated with enhanced levels of gene expression for several different genes in monocots (Callis et al., 1987; Luehrsen and Walbot, 1991). For these monocot genes, deletion of the intron does not influence expression levels when the gene is placed in dicot cells. Roles of intron sequences in expression of genes for dicot species are less clear cut. The polyubiquitin genes of Arabidopsis contain an intron that is reported to enhance expression levels in transient assays (Norris et al., 1993); however, for expression of the polyubiquitin gene from *Nicotiana tabacum*, the similarly positioned intron is apparently dispensable (Genschik et al., 1994). In potato, the sucrose synthase genes *Sus3* and *Sus4* each contain an intron in their 5′ leader that has been shown to be essential for normal developmental regulation (Fu et al., 1995a, 1995b). However, normal expression of many dicot genes has been shown to require only upstream sequences, including the Arabidopsis MADS box gene *APETALA3* (Jack et al., 1994).

The homolog of *AG* from Antirrhinum, *PLENA* (*PLE*), has a genomic organization that is nearly identical to that of *AG* (Bradley et al., 1993). Two classes of mutant alleles have been identified: recessive (*ple*) alleles show an *ag*-like phenotype, with indeterminate flowers composed solely of sepals and petals, whereas semidominant (*ovulata*) alleles show homeotic conversions of the first-whorl sepals to carpels and of the second-whorl petals to stamens. Consistent with the ABC model for floral organ specification (reviewed in Weigel and Meyerowitz, 1994), ectopic expression of *PLE* in the outer two whorls (and vegetative parts of the plant) has been observed in plants with the *ovulata* phenotype. Both of these two complementary phenotypes arise from *TAM3* transposable element insertions into the large second intron (Bradley et al., 1993).

Two general models to account for the alternative phenotypes feature either the disruption of *cis*-acting elements essential for normal expression located within the large second intron or influences on *PLE* expression derived from the transposon itself. The demonstration that the recessive *ple*-type alleles have *TAM3* inserted so that transcription would occur in the same orientation as the gene and that the dominant *ovulata*-type alleles carry *TAM3* insertions in the opposite orientation supports a role for transposon structure or activity in the mutant phenotypes.

We have shown that intragenic sequences are essential for normal *AG* expression. In Arabidopsis, loss of this region results in both loss of negative control over spatial distribution of expression (both floral and vegetative) and loss of positive regulation, especially activation in the floral meristem. Recently, using similar approaches, we have shown that essential intragenic *cis* sequences are restricted to the second large intron (M.K. Deyholos and L.E. Sieburth, manuscript in preparation). A comparison of the large introns of *AG* and *PLE* show dozens of short stretches (up to 12 nucleotides) of sequence identity throughout the large second intron. The potential significance of these alignments is unclear. These large introns are highly AT rich (72% for *AG* and 70% for *PLE*), and the precise positions of *TAM3* insertions that cause the *ovulata* phenotype in Antirrhinum have not been reported. Future dissection of the intragenic control region of *AG* should provide insights into *AG* regulatory circuits, and comparisons with Antirrhinum may provide insights into aspects of these regulatory circuits that are conserved between these two divergent angiosperm species.

METHODS

AGAMOUS::β-Glucuronidase Gene Fusion Constructs

Two constructs that fused portions of *AGAMOUS* (*AG*) to β-glucuronidase (*GUS*) were constructed using a polymerase chain reaction (PCR)–mediated fusion strategy. First, *GUS* and portions of *AG* were amplified using oligonucleotides that conferred ~30 bp of overlap to the two initial products. A second round of amplification using the two initial products and the two outer oligonucleotides generated the final fused product. Specifically, for pAG::*GUS*, the initial *AG* product was amplified from plasmid pBS-5104 (described below) by using oligonucleotides AG-GUS2 5′-GGACGTAACATTGGGGGGAGAAGAACAA-3′ (underlined portions of oligonucleotides indicate the region containing homology to the *GUS* coding region) and LS106 5′-TAACTTCCTTAATTAGTGAAAC-3′. The initial *GUS* fragment was amplified from the pBI221 plasmid (Clontech, Palo Alto, CA) by using oligonucleotides AG-GUS1 5′-CTCCCCCCAATGTTACGTCCTGTAGAAAC-3′ and the M13 reverse primer. The two initial PCR products were mixed, and the fusion product was obtained by amplifying with only oligonucleotides for LS106 and M13 reverse primer. This fusion product was assembled with an additional 6 kb of the upstream region of *AG* obtained from clone pBS5104. The fusion product was cloned into the plant transformation vector pCGN1547 (McBride and Summerfelt, 1990) as an Asp718 fragment.

The second *AG*::*GUS* fusion was constructed with the fusion site at the beginning of the third exon. PCR-mediated gene fusion was performed as given above, except that oligonucleotides AgGUS4 5′-GACGTAACATACTGCAATAGTTTTTAAG-3′ and AgSeq-25 5′-TTTAGTACGGATCCAATAG-3′ were used to amplify the *AG* portion from the cosmid pCIT540 (Yanofsky et al., 1990). Oligonucleotides for AgGUS3 5′-AACTATTGCAGTATGTTACGTCCTGTAG-3′ and the M13 reverse primer were used to amplify the *GUS* coding region. The fusion product was assembled in the plant transformation vector pCGN1547 with the same upstream region of *AG* used in the pAG::*GUS* fusion. This fusion product also included the genomic region between the first and the third exons. The upstream region of *AG* was obtained from pLAGE13, which is an EcoRI subclone from cosmid N71 (from G. Drews, University of Utah, Salt Lake City). Linkers were used to convert the XbaI site ~5.5 kb upstream of the PstI site to Asp718. The 4-kb PstI-HindIII fragment was purified from cosmid pCIT540. These two fragments were ligated into the Asp718 and BamHI sites of pBluescript SK+ (Stratagene, La Jolla, CA) to make pBS-5104.

Plant Transformation

Lines of transgenic plants carrying each construct were established using *Agrobacterium tumefaciens*–mediated transformation. Root tissue of the *Arabidopsis thaliana* ecotype Nossen (No-0) was cultured in liquid medium and used for transformation after established protocols (Valvekens et al., 1988). The insert copy number has been assessed by analysis of kanamycin resistance segregation.

GUS Staining

Tissue for GUS staining was gently fixed by incubation in 90% acetone, on ice, for 15 to 20 min and then rinsed in 50 mM $NaPO_4$, pH 7.2, 0.5 mM $K_3Fe(CN)_6$, and 0.5 mM $K_4Fe(CN)_6$. The tissue was then placed in staining solution (50 mM $NaPO_4$, pH 7.2, 2 mM X-gluc [Gold Biotechnology, St. Louis, MO], 0.5 mM $K_3Fe[CN]_6$, and 0.5 mM $K_4Fe[CN]_6$), vacuum infiltrated, and incubated at 37°C overnight. After staining, the tissue was processed through an ethanol series (30, 50, 70, 85, 95, 100, and 100%), with the 50% step of the series replaced by a 1-hr formaldehyde–acetic acid fixation (50% ethanol, 5% acetic acid, and 3.7% formaldehyde). To prepare tissue for histological analysis, we passed tissue through a xylene series and embedded it in Paraplast (Sigma). Sections (10 μm) were cut from the embedded tissue, wax was removed by a brief incubation in xylene, and sections were mounted in Paraplast. Sections were visualized using dark-field illumination.

Image Processing

Slides were scanned using a Coolscan (Nikon, Inc., Melville, NY), with brightness and contrast adjusted with Adobe Photoshop 2.5 (Mountain View, CA). Figures 2 to 6 were printed using a digital printer (model XLS 8300; Eastman Kodak, Rochester, NY).

Plant Material

All plants were grown in constant light at 25°C in a 1:1:1 mix of vermiculite, perlite, and potting soil. Transgenic seeds were selected by germination on medium containing a 0.5 × Murashige and Skoog basal salt mixture (Sigma), 50 μg/mL kanamycin, and 0.7% phytagar (Gibco BRL, Grand Island, NY). Approximately 8 days after germination, transgenic seedlings were identified by their long roots and production of green true leaves.

ACKNOWLEDGMENTS

We thank Justin Goodrich for allowing us to use *clf-2*, Esther Koh for her assistance with plant transformations, Gary Drews for the plas-

mid pLAGE-13, Zhongchi Liu for use of *lug-3*, Michael Deyholos for assistance in sequence comparisons, and Mike Frohlich for assistance with the initial analysis of these floral mutant lines. This work was supported by a Damon Runyon–Walter Winchell Cancer Research Fellowship (Grant No. DRG1081 to L.E.S.) and by the National Institutes of Health (Grant No. GM45697 to E.M.M.).

Received November 1, 1996; accepted January 16, 1997.

REFERENCES

Bowman, J.L., Smyth, D.R., and Meyerowitz, E.M. (1989). Genes directing flower development in *Arabidopsis.* Plant Cell **1,** 37–52.

Bowman, J.L., Drews, G.N., and Meyerowitz, E.M. (1991). Expression of the Arabidopsis floral homeotic gene *AGAMOUS* is restricted to specific cell types late in flower development. Plant Cell **3,** 749–758.

Bradley, D., Carpenter, R., Sommer, H., Hartley, N., and Coen, E. (1993). Complementary floral homeotic phenotypes result from opposite orientations of a transposon at the *plena* locus of Antirrhinum. Cell **72,** 85–95.

Callis, J., Fromm, M., and Walbot, V. (1987). Introns increase gene expression in cultured maize cells. Genes Dev. **1,** 1183–1200.

Coupland, G., Dash, S., Goodrich, J., Lee, K., Long, D., Martin, M., Puangsomlee, P., Putterill, J., Robson, F., and Wilson, K. (1993). Molecular and genetic analysis of the control of flowering time in response to daylength in *Arabidopsis thaliana.* Plant Flowering Newslett. **16,** 27–32.

Dietrich, R.A., Radke, S.E., and Harada, J.J. (1992). Downstream DNA sequences are required to activate a gene expressed in the root cortex of embryos and seedlings. Plant Cell **4,** 1371–1382.

Dougherty, W.G., and Parks, T.D. (1995). Transgenes and gene suppression: Telling us something new? Curr. Opin. Cell Biol. **7,** 399–405.

Drews, G.N., Bowman, J.L., and Meyerowitz, E.M. (1991). Negative regulation of the Arabidopsis homeotic gene *AGAMOUS* by the *APETALA2* product. Cell **65,** 991–1002.

Fu, H., Kim, S.Y., and Park, W.D. (1995a). High-level tuber expression and sucrose inducibility of a potato *Sus4* sucrose synthase gene require 5′ and 3′ flanking sequences and the leader intron. Plant Cell **7,** 1387–1394.

Fu, H., Kim, S.Y., and Park, W.D. (1995b). A potato *Sus3* sucrose synthase gene contains a context-dependent 3′ element and a leader intron with both positive and negative tissue-specific effects. Plant Cell **7,** 1395–1403.

Genschik, P., Marbach, M., Uze, M., Feuerman, M., Plesse, B., and Fleck, J. (1994). Structure and promoter activity of a stress and developmentally regulated polyubiquitin-encoding gene of *Nicotiana tabacum.* Gene **148,** 195–202.

Gremke, L., Lord, P.C.W., Sabacan, L., Lin, S.-C., Wohlwill, A., and Storti, R.V. (1993). Coordinate regulation of *Drosophila Tropomyosin* gene expression is controlled by multiple muscle-type–specific positive and negative enhancer elements. Dev. Biol. **159,** 513–527.

Hinz, U., Wolk, A., and Renkawitz-Pohl, R. (1992). Ultrabithorax is a regulator of β3 tubulin expression in the Drosophila visceral mesoderm. Development **116,** 543–554.

Jack, T., Fox, G.L., and Meyerowitz, E.M. (1994). Arabidopsis homeotic gene *APETALA3* ectopic expression: Transcriptional and post-transcriptional regulation determine floral organ identity. Cell **76,** 703–716.

Jefferson, R.A., Kavanagh, T.A., and Bevan, M.W. (1987). GUS fusions: β-Glucuronidase as a sensitive and versatile gene fusion marker in higher plants. EMBO J. **6,** 3901–3907.

Larkin, J.C., Oppenheimer, D.G., Pollock, S., and Marks, M.D. (1993). Arabidopsis *GLABROUS1* gene requires downstream sequences for function. Plant Cell **5,** 1739–1748.

Liu, Z., and Meyerowitz, E.M. (1995). *LEUNIG* regulates *AGAMOUS* expression in Arabidopsis flowers. Development **121,** 975–991.

Luehrsen, K.R., and Walbot, V. (1991). Intron enhancement of gene expression and the splicing efficiency of introns in maize cells. Mol. Gen. Genet. **225,** 81–93.

Mandel, A.M., Bowman, J.L., Kempin, S.A., Ma, H., Meyerowitz, E.M., and Yanofsky, M.F. (1992). Manipulation of flower structure in transgenic tobacco. Cell **71,** 133–143.

McBride, K.E., and Summerfelt, K.R. (1990). Improved binary vectors for *Agrobacterium*-mediated plant transformation. Plant Mol. Biol. **14,** 269–276.

Mizukami, Y., and Ma, H. (1992). Ectopic expression of the floral homeotic gene *AGAMOUS* in transgenic Arabidopsis plants alters floral organ identity. Cell **71,** 119–131.

Modrusan, Z., Reiser, L., Feldmann, K.A., Fischer, R.L., and Haughn, G.W. (1994). Homeotic transformation of ovules into carpel-like structures in Arabidopsis. Plant Cell **6,** 333–349.

Norris, S.R., Meyer, S.E., and Callis, J. (1993). The intron of *Arabidopsis thaliana* polyubiquitin genes is conserved in location and is a quantitative determinant of chimeric gene expression. Plant Mol. Biol. **21,** 895–906.

Ray, A., Robinson-Beers, K., Ray, S., Baker, S.C., Lang, J.D., Preuss, D., Milligan, S.B., and Gasser, C.S. (1994). *Arabidopsis* floral homeotic gene *BELL* (*BEL1*) controls ovule development through negative regulation of *AGAMOUS* gene (*AG*). Proc. Natl. Acad. Sci. USA **91,** 5761–5765.

Reiser, L., Modrusan, Z., Margossian, L., Samach, A., Ohad, N., and Haughn, G.W. (1995). The *BELL1* gene encodes a homeodomain protein involved in pattern formation. Cell **83,** 735–742.

Smyth, D.R., Bowman, J.L., and Meyerowitz, E.M. (1990). Early flower development in *Arabidopsis.* Plant Cell **2,** 755–767.

Valvekans, D., Van Montagu, M., and Van Lijsebettens, M. (1988). *Agrobacterium tumefaciens*–mediated transformation of *Arabidopsis thaliana* root explants by using kanamycin selection. Proc. Natl. Acad. Sci. USA **85,** 5536–5540.

Weigel, D., and Meyerowitz, E.M. (1993). Activation of floral homeotic genes in Arabidopsis. Science **261,** 1723–1726.

Weigel, D., and Meyerowitz, E.M. (1994). The ABCs of floral homeotic genes. Cell **78,** 203–209.

Yanofsky, M.F., Ma, H., Bowman, J.L., Drews, G.N., Feldmann, K.A., and Meyerowitz, E.M. (1990). The protein encoded by the *Arabidopsis* homeotic gene *agamous* resembles transcription factors. Nature **346,** 35–39.